



ELSEVIER

Available online at www.sciencedirect.com

SCIENCE @ DIRECT®

Journal of Computational Physics 195 (2004) 773–789

JOURNAL OF
COMPUTATIONAL
PHYSICS

www.elsevier.com/locate/jcp

The finite element method with weighted basis functions for singularly perturbed convection–diffusion problems

Xiang-Gui Li ^{a,*}, C.K. Chan ^b, Song Wang ^c

^a *Beijing Information Technology Institute, Beijing 100101, PR China*

^b *Department of Applied Mathematics, The Hong Kong Polytechnic University, Kowloon, Hong Kong*

^c *School of Mathematics and Statistics, The University of Western Australia, Perth, Australia*

Received 10 July 2003; received in revised form 15 October 2003; accepted 15 October 2003

Abstract

In this paper, we present a finite element method for singularly perturbed convection–diffusion problems in both one and two dimensions, based on a set of weighted basis functions constructed on unstructured meshes (in 2D). For the one-dimensional case, both first and second-order schemes are discussed. A technique for approximating fluxes is proposed. Some theoretical results on uniform convergence are obtained. For the two-dimensional case, a first-order scheme is constructed for problems with two singular perturbation parameters. A technique is also developed in approximating fluxes in 2D. This technique is used to simplify the calculation of the integrals in the stiffness matrix arising from the scheme, which will save computational costs. The numerical results support the theoretical results and demonstrate that the method is stable for a wide range of singular perturbation parameters.

© 2003 Elsevier Inc. All rights reserved.

Keywords: Singular perturbation; Convection–diffusion equations; Finite element method; Flux approximation; Unstructured mesh

1. Introduction

Many phenomena in engineering, physics and finance are governed by convection–diffusion equations in which the magnitudes of the diffusion coefficients are much smaller than those of the convection coefficients. Such problems are called convection-dominated or singularly perturbed, and boundary layers normally appear in the solution. Due to the presence of boundary layers, standard finite element or finite difference methods are, in general, not suitable for solving these problems, because these methods will result in spurious oscillations or non-physical solutions. To overcome this difficulty, many special finite element techniques have been developed. These include upwind finite element [2,3,5,6,9–11,14],

* Corresponding author. Present address: Department of Applied Mathematics, University of Petroleum, Taian, Dongying 257062, China. Tel.: +852-27666919; fax: +852-23629045.

E-mail addresses: xianggui-li@vip.sina.com (X.-G. Li), ck.chan@polyu.edu.hk (C.K. Chan), swang@maths.uwa.edu.au (S. Wang).

Petrov–Galerkin finite element [4,13], streamline diffusion methods [15,16], monotone finite element [29] and exponentially fitted finite element [12,18–20,26–28]. However, the former three methods do not always give accurate results, especially when the diffusion coefficients are of the same magnitude as that of the mesh size used. The exponentially fitted methods in [26,27] do not have explicit expressions for the basis functions and they are essentially first-order schemes. Thus, we are motivated to look for explicit basis functions, which are convenient to construct and analyze, and easy to extend to high-order and/or multi-dimensional cases.

In this paper, we present a novel finite element method for a singularly perturbed convection–diffusion problem in one and two dimensions. This method is based on a set of basis functions obtained by multiplying a standard basis function constructed on a triangular mesh (2D case) by a suitable weight. This finite element method always results in non-oscillatory numerical solutions. The paper is organized as follows.

The weighted basis functions in one dimension are described in the next section. Both first and second-order schemes in one dimension are presented and analyzed in Section 3. In Section 4, we shall discuss the method on an unstructured triangular mesh in two dimensions. Numerical results are presented in Section 5 to demonstrate the effectiveness and usefulness of this method.

In what follows we will use the conventional notation for function sets and spaces. In particular, we will use $L^2(S)$ and $C^k(S)$ to denote, respectively, the space of square integrable functions and the set of k th continuously differentiable functions on the set S .

2. 1D weighted basis functions

In this section, we consider the 1D linear singularly perturbed problem

$$(-\varepsilon w' + b(x)w)' + c(x)w = f(x), \quad w(0) = w(1) = 0, \quad (2.1)$$

where $0 < \varepsilon \ll 1$, $c(x) \geq 0$, and $b(x)$ has a positive lower bound. In this case the problem has a boundary layer at $x = 1$, see [17,22].

To be more precise, we assume that $b(x), c(x), f(x) \in C^1([0, 1])$ and

$$0 < \alpha \leq b(x) \leq \beta \quad \text{for } x \in [0, 1], \quad (2.2)$$

for some positive constants α and β . The above conditions guarantee the existence of a unique solution $w \in C^2([0, 1])$.

Let

$$\varpi = \{x_i \mid 0 = x_0 < x_1 < \cdots < x_{N-1} < x_N = 1\}$$

be a non-uniform mesh on $[0, 1]$. We put $I_i := (x_{i-1}, x_i)$ and $h_i := x_i - x_{i-1}$ for $i = 1, 2, \dots, N$. The mesh parameter, h , is defined by $h = \max_{1 \leq i \leq N} h_i$.

On this partition, the conventional piecewise linear basis functions satisfy the following:

$$\varphi_i(x_l) = 1, \quad \varphi_i(x_l) = 0 (l \neq i), \quad i = 1, 2, \dots, N-1. \quad (2.3)$$

The second-order finite element space can be obtained by adding the following bubble functions:

$$\psi_i = \begin{cases} (x - x_{i-1})(x - x_i)/h_i & \text{if } x \in I_i, \\ 0 & \text{otherwise.} \end{cases} \quad (2.4)$$

For $i = 1, 2, \dots, N - 1$, let $m_i(x)$ be a positive function. We define a new set of basis functions as

$$\tilde{\varphi}_i = \begin{cases} \frac{m_i(x)}{m_i(x)\varphi_i + m_{i-1}(x)\varphi_{i-1}} \varphi_i, & x \in I_i, \\ \frac{m_i(x)}{m_i(x)\varphi_i + m_{i+1}(x)\varphi_{i+1}} \varphi_i, & x \in I_{i+1}, \\ 0, & \text{otherwise,} \end{cases} \tag{2.5}$$

for $i = 1, \dots, N - 1$. The basis functions corresponding to the two end points are $\varphi_0 = (x_1 - x)/h_1$ and $\varphi_N = (x - x_{N-1})/h_N$.

The choice of the weighting function $m_i(x)$ in (2.5) is rather arbitrary, but we choose it as the following exponentially fitted spline:

$$m_i(x) = B[-b(x)(x - x_i)/\varepsilon],$$

where $B(z)$ is the Bernoulli function defined by

$$B(z) = \begin{cases} \frac{z}{e^z - 1} & \text{if } z \neq 0, \\ 1, & \text{if } z = 0. \end{cases}$$

To obtain the stability of standard finite element approximation of convection dominated diffusion equations, an exponentially decreasing weight only in the layer elements was also introduced by Axelsson [1]. By adding more basis functions, we can obtain higher order basis functions. For example, the second order basis functions can be obtained by adding the following basis functions to the set defined by (2.5).

$$\begin{aligned} \tilde{\psi}_i &= (x - x_i)\tilde{\varphi}_i \quad \text{for } i = 1, \dots, N - 1, \quad x \in I_i \cup I_{i+1}, \\ \tilde{\psi}_0 &= \frac{m_0(x)\varphi_0}{m_0(x)\varphi_0 + m_1(x)\varphi_1} (x - x_0), \quad x \in I_1, \end{aligned} \tag{2.6}$$

Typical cases of basis functions $\tilde{\varphi}_i$ and $\tilde{\psi}_i$ are illustrated in Figs. 1 and 2.

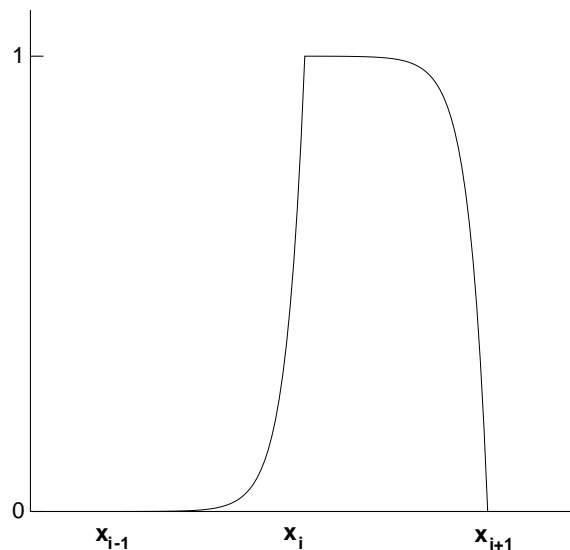


Fig. 1. An example of the basis function $\tilde{\varphi}_i(x)$.

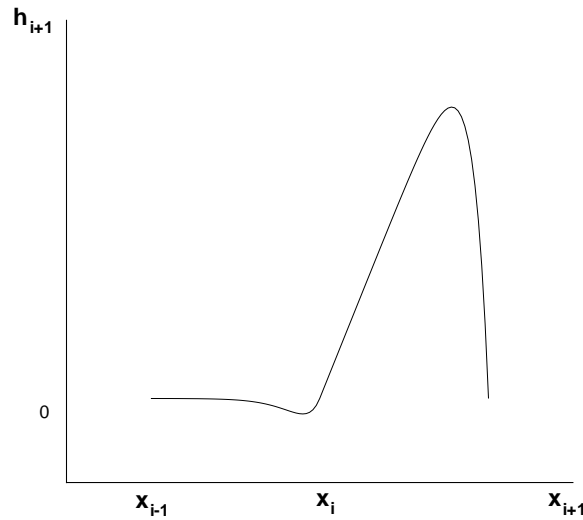


Fig. 2. An example of the basis function $\tilde{\psi}_i(x)$.

Remark 2.1. If $b(x) = 0$ or the weights m_i ($i = 1, 2, \dots, N - 1$) are identical, the weighted basis functions reduce to piecewise polynomial basis functions in the standard finite element method. Furthermore, when ε tends to 0, the limits of $\tilde{\varphi}_i$ and $\tilde{\psi}_i$ become discontinuous, and they are similar to the basis functions of the local discontinuous Galerkin method used in [7,8] for conservation laws and nonlinear time-dependent convection–diffusion systems.

Lemma 2.1. The basis functions $\tilde{\varphi}_i$ and $\tilde{\psi}_i$ satisfy

$$\begin{aligned} \tilde{\varphi}_i(x_i) &= 1, \quad \tilde{\varphi}_i(x_j) = 0 (j \neq i), \quad 0 \leq \tilde{\varphi}_i \leq 1, \\ \tilde{\psi}_i(x_j) &= 0, \quad j = 0, 1, \dots, N. \end{aligned} \tag{2.7}$$

Furthermore, we have for $i = 2, \dots, N - 1$,

$$\tilde{\varphi}_{i-1}(x) + \tilde{\varphi}_i(x) = 1 \quad \forall x \in I_i, \tag{2.8}$$

and for $i = 1, \dots, N$,

$$\tilde{\psi}_{i-1}(x) + \tilde{\psi}_i(x) = (x - x_i) + h_i \tilde{\varphi}_{i-1}(x), \quad x \in I_i. \tag{2.9}$$

Proof. Properties (2.7) and (2.8) can be trivially proved by using (2.3) and (2.4). In what follows we only show (2.9). From the definition of $\tilde{\psi}_i(x)$ in (2.6), we have

$$\tilde{\psi}_{i-1}(x) + \tilde{\psi}_i(x) = (x - x_{i-1})\tilde{\varphi}_{i-1} + (x - x_i)\tilde{\varphi}_i.$$

Substituting (2.5) into the above equality, we have that for $x \in I_i$,

$$\begin{aligned} \tilde{\psi}_{i-1}(x) + \tilde{\psi}_i(x) &= (x - x_{i-1}) \frac{m_{i-1}(x)}{m_i(x)\varphi_i + m_{i-1}(x)\varphi_{i-1}} \varphi_{i-1} + (x - x_i) \frac{m_i(x)}{m_i(x)\varphi_i + m_{i-1}(x)\varphi_{i-1}} \varphi_i \\ &= (x - x_i) + h_i \tilde{\varphi}_{i-1}. \end{aligned}$$

This completes the proof of the lemma. \square

Note that if $m_k(x)$, $k = i - 1, i, i + 1$ are identical, we have

$$\begin{aligned} \tilde{\varphi}_i(x) &= \varphi_i(x), \\ \tilde{\psi}_i(x) &= \psi_i(x) - \psi_{i+1}(x). \end{aligned} \tag{2.10}$$

In general, if $m_k(x)$, $k = i - 1, i, i + 1$ are not identical, the statement (2.10) does not hold. However, on $I_i \cup I_{i+1}$, we still have

$$P_1 \subset \text{Span}\{\tilde{\varphi}_{i+1}, \tilde{\psi}_{i+1}, \tilde{\varphi}_i, \tilde{\psi}_i, \tilde{\varphi}_{i-1}, \tilde{\psi}_{i-1}\},$$

where P_1 denotes the set of all piecewise linear polynomials on $I_i \cup I_{i+1}$.

We now consider the approximation of fluxes. By direct computation, we get

$$\begin{aligned} \tilde{\varphi}'_i(x)|_{I_i} &= -\frac{b}{\varepsilon} \frac{e^{b(x-x_i)/\varepsilon}}{e^{-bh_i/\varepsilon} - 1} - \frac{b'}{\varepsilon} \frac{(e^{b(x-x_i)/\varepsilon} - 1)e^{-bh_i/\varepsilon}h_i + (e^{-bh_i/\varepsilon} - 1)e^{b(x-x_i)/\varepsilon}(x-x_i)}{(e^{-bh_i/\varepsilon} - 1)^2}, \\ \tilde{\varphi}'_i(x)|_{I_{i+1}} &= -\frac{b}{\varepsilon} \frac{e^{b(x-x_i)/\varepsilon}}{e^{bh_{i+1}/\varepsilon} - 1} + \frac{b'}{\varepsilon} \frac{(e^{b(x-x_i)/\varepsilon} - 1)e^{bh_{i+1}/\varepsilon}h_{i+1} - (e^{bh_{i+1}/\varepsilon} - 1)e^{b(x-x_i)/\varepsilon}(x-x_i)}{(e^{bh_{i+1}/\varepsilon} - 1)^2}. \end{aligned} \tag{2.11}$$

Let $g_i(x)$ and $h_i(x)$ denote the flux associated with $\tilde{\varphi}_i(x)$ and $\tilde{\psi}_i(x)$, respectively, i.e.,

$$\begin{aligned} g_i(x) &= -\varepsilon\tilde{\varphi}'_i(x) + b(x)\tilde{\varphi}_i(x), \\ h_i(x) &= -\varepsilon\tilde{\psi}'_i(x) + b(x)\tilde{\psi}_i(x). \end{aligned}$$

Substituting (2.5), (2.6) and (2.11) into the above, we obtain

$$g_i(x) = \bar{g}_i(x) + b'R_i(x), \tag{2.12}$$

$$h_i(x) = \bar{h}_i(x) + b'(x-x_i)R_i(x), \tag{2.13}$$

where

$$\bar{g}_i(x) = \begin{cases} b \frac{e^{-bh_i/\varepsilon}}{e^{-bh_i/\varepsilon} - 1}, & x \in I_i, \\ b \frac{e^{bh_{i+1}/\varepsilon}}{e^{bh_{i+1}/\varepsilon} - 1}, & x \in I_{i+1}, \\ 0, & \text{otherwise,} \end{cases} \tag{2.14}$$

$$\bar{h}_i(x) = (x-x_i)\bar{g}_i(x) - \varepsilon\tilde{\varphi}_i(x),$$

and

$$R_i(x) = \begin{cases} \frac{(e^{b(x-x_i)/\varepsilon} - 1)e^{-bh_i/\varepsilon}h_i + (e^{-bh_i/\varepsilon} - 1)e^{b(x-x_i)/\varepsilon}(x-x_i)}{(e^{-bh_i/\varepsilon} - 1)^2}, & x \in I_i, \\ -\frac{(e^{b(x-x_i)/\varepsilon} - 1)e^{bh_{i+1}/\varepsilon}h_{i+1} - (e^{bh_{i+1}/\varepsilon} - 1)e^{b(x-x_i)/\varepsilon}(x-x_i)}{(e^{bh_{i+1}/\varepsilon} - 1)^2}, & x \in I_{i+1}, \\ 0, & \text{otherwise.} \end{cases}$$

Using the definition of $\tilde{\varphi}_i$ in (2.5) we can show that $\bar{g}_i(x)$ in (2.14) can be rewritten as

$$\bar{g}_i(x) = \frac{-\varepsilon}{x-x_k} B\left(\frac{b}{\varepsilon}(x-x_k)\right) \tilde{\varphi}_i, \tag{2.15}$$

where $k = i - 1$ if $x \in I_i$ and $k = i + 1$ when $x \in I_{i+1}$.

From (2.12), we see that the flux $g_i(x)$ can be decomposed into a leading term $\bar{g}_i(x)$ and a remainder term $b'R_i(x)$. Here $R_i(x_{i-1}) = R(x_i) = R(x_{i+1}) = 0$. Using (2.14), we get that for $x \in I_{i+1}$

$$|b'R_i(x)| \leq \left| \frac{b'}{b} \bar{g}_i(x) \right| h.$$

Following the above analysis, one obtains that for $x \in I_{i+1}$,

$$\bar{g}_i(x) + \bar{g}_{i+1}(x) = b(x),$$

$$g_i(x) + g_{i+1}(x) = b(x),$$

$$R_i(x) + R_{i+1}(x) = 0.$$

3. Finite element method in one dimension

Let $V_h = \text{Span}\{\tilde{\psi}_i\}$. We define the following Galerkin finite element problem: find a $w_h \in V_h$ such that $\forall v_h \in V_h$, we have

$$-(-\varepsilon w'_h + b(x)w_h, v'_h) + (c(x)w_h, v_h) = (f, v_h), \tag{3.1}$$

where (\cdot, \cdot) denotes the inner product.

3.1. First-order scheme

We first consider the first-order scheme. Setting $w_h = \sum_{j=1}^{N-1} w_j \tilde{\varphi}_j$ and $v_h = \tilde{\varphi}_i$ for any $i = 1, \dots, N - 1$ in (3.1), we obtain

$$q_{i+1}w_{i+1} + q_iw_i + q_{i-1}w_{i-1} = (f, \tilde{\varphi}_i) \tag{3.2}$$

with the boundary conditions $w_0 = 0 = w_N$, where

$$q_k = \int_{x_{i-1}}^{x_{i+1}} [-g_k(x)\tilde{\varphi}'_i(x) + c(x)\tilde{\varphi}_k\tilde{\varphi}_i]dx, \quad k = i + 1, i, i - 1. \tag{3.3}$$

As $|R_k(x)| = O(h)$, $g_k(x)$ can be approximated by $\bar{g}_k(x)$. So we have

$$q_i \simeq - \left(\int_{x_{i-1}}^{x_i} b \frac{e^{-bh_i/\varepsilon}}{e^{-bh_i/\varepsilon} - 1} \varphi'_i dx + \int_{x_i}^{x_{i+1}} b \frac{e^{bh_{i+1}/\varepsilon}}{e^{bh_{i+1}/\varepsilon} - 1} \varphi'_i dx \right) + \int_{x_{i-1}}^{x_{i+1}} c(x)\tilde{\varphi}_i\tilde{\varphi}_i dx.$$

Noticing the fact $b(x) > \alpha$ from (2.2) and using (2.7), we immediately obtain

$$\begin{aligned} q_i &\simeq - \left[\bar{g}_i(x_i^-) \int_{x_{i-1}}^{x_i} \varphi'_i dx + \bar{g}_i(x_{i+1}^-) \int_{x_i}^{x_{i+1}} \varphi'_i dx \right] + \int_{x_{i-1}}^{x_{i+1}} c(x)\tilde{\varphi}_i\tilde{\varphi}_i dx \\ &= -\bar{g}_i(x_i^-) + \bar{g}_i(x_{i+1}^-) + \int_{x_{i-1}}^{x_{i+1}} c(x)\tilde{\varphi}_i\tilde{\varphi}_i dx. \end{aligned}$$

Here $\bar{g}(x_i^-) = \lim_{x \rightarrow 0^-} \bar{g}(x)$. Analogously to the above deduction, we have

$$q_{i+1} = \bar{g}_{i+1}(x_{i+1}^-) + \int_{x_i}^{x_{i+1}} c(x) \tilde{\varphi}_{i+1} \tilde{\varphi}_i dx,$$

$$q_{i-1} = -\bar{g}_{i-1}(x_i^-) + \int_{x_{i-1}}^{x_i} c(x) \tilde{\varphi}_{i-1} \tilde{\varphi}_i dx.$$

For the case when $\varepsilon \ll h$, we use $\bar{g}_i(x)$ to approximate $g_i(x)$ so that the computational cost is reduced. If the mesh size h has the same magnitude as ε , it is not necessary to replace the flux $g_i(x)$ by $\bar{g}_i(x)$ because $g_i(x)$ is very smooth and integrals in (3.3) are easy to evaluate.

Scheme (3.2) is similar to that obtained by Stynes and O’Riordan [23,24] by applying the finite element method with exponentially fitted splines to (2.1). In [23,24], frozen coefficients for $b(x)$ and $c(x)$ are adopted. Using the analogous strategy as in [24,25], we can prove the following theorem. Here we omit the repeating proof.

Theorem 3.1. *Let w and w_h be solutions to (2.1) and (3.2), respectively. Then, we have*

$$\|w - w_h\|_e \leq c_1 h^{1/2},$$

where c_1 is a positive constant independent of h , w and ε , and $\|v\|_e = \varepsilon(v', v') + (v, v)$.

3.2. Second-order scheme

Let $w_h = \sum_{j=1}^{N-1} w_j \tilde{\varphi}_j + \sum_{j=0}^{N-1} v_j \tilde{\psi}_j$ and $v_h = \tilde{\varphi}_i (i = 1, \dots, N - 1), \tilde{\psi}_i (i = 0, \dots, N - 1)$ in (3.1), we obtain

$$q_{i+1} w_{i+1} + q_i w_i + q_{i-1} w_{i-1} + p_{i+1} v_{i+1} + p_i v_i + p_{i-1} v_{i-1} = (f, \tilde{\varphi}_i), \tag{3.4}$$

$$r_{i+1} w_{i+1} + r_i w_i + r_{i-1} w_{i-1} + s_{i+1} v_{i+1} + s_i v_i + s_{i-1} v_{i-1} = (f, \tilde{\psi}_i), \tag{3.5}$$

for $i = 1, 2, \dots, N - 1$, and

$$r_1 w_1 + s_1 v_1 + s_0 v_0 = (f, \tilde{\psi}_0). \tag{3.6}$$

In (3.4)–(3.6), the coefficients $q_k (k = i - 1, i, i + 1)$ are determined by (3.3) and the others are defined by

$$p_k = \int_{x_{i-1}}^{x_{i+1}} [(e \tilde{\psi}'_k - b(x) \tilde{\psi}_k) \tilde{\varphi}'_i(x) + c(x) \tilde{\psi}_k \tilde{\varphi}_i] dx,$$

$$r_k = \int_{x_{i-1}}^{x_{i+1}} [(e \tilde{\varphi}'_k - b(x) \tilde{\varphi}_k) \tilde{\psi}'_i(x) + c(x) \tilde{\varphi}_k \tilde{\psi}_i] dx,$$

$$s_k = \int_{x_{i-1}}^{x_{i+1}} [(e \tilde{\psi}'_k - b(x) \tilde{\psi}_k) \tilde{\psi}'_i(x) + c(x) \tilde{\psi}_k \tilde{\psi}_i] dx,$$

for $k = i + 1, i, i - 1$.

Remark 3.1. We comment that, as shown by Roos [21], even on a Shishkin mesh, stability of a numerical solution obtained by conventional finite element is very sensitive to the choice of the boundary layer thickness $\tau_0 \varepsilon \ln N$, where τ_0 is a positive parameter characterizing the width of the layer. However, if we discretize (2.1) by the finite element method with weighted basis functions in a subregion containing the boundary layer and by the standard finite element method in the rest of computational domain, the resulting numerical solutions are satisfactory and insensitive to τ_0 . This will be demonstrated later in Fig. 4.

Remark 3.2. We also comment that it is possible to extend this second-order scheme to two dimensions. However, the discussion of this extension is lengthy, and thus we will omit it. In practice, the integrals defining p_k, r_k and s_k given in the above have to be approximated by a quadrature rule. Attention needs to be paid to this approximation when $\varepsilon \ll 1$ in order not to affect the second-order accuracy of the scheme. This is because all the basis functions contain layers when ε is small. Nevertheless, it is possible to find approximations to these integrals. For example, since $\tilde{\varphi}_i$ behaves like a step function when $\varepsilon \ll 1$ (cf. Fig. 1), $\tilde{\varphi}'_i$ behaves like a δ -function. We may use this information to approximate the first term in p_k . We will leave this discussion, along with the extension of the second-order scheme to higher dimensions, to a forthcoming paper.

4. Finite element method in two dimensions

Let us consider the following problem in two-dimensional space:

$$\begin{aligned} \nabla \cdot (-A_\varepsilon \nabla w + \mathbf{b}w) + \lambda w &= f(X), \quad X \in \Omega \subset \mathbb{R}^2, \\ w|_{\partial\Omega} &= 0, \end{aligned} \quad (4.1)$$

where Ω is a bounded open set, $\partial\Omega$ denotes the boundary of Ω , $A_\varepsilon = \text{diag}\{\varepsilon_1, \varepsilon_2\}$, $X = (x, y)^t$ and $\mathbf{b} = (b_1(X), b_2(X))^t$. Eq. (4.1) is well-posed if

$$\frac{1}{2} \nabla \cdot \mathbf{b}(x, y) + \lambda(x, y) > 0 \quad (4.2)$$

for $X \in \Omega$. For the convection coefficients in (4.1), we assume that $b_1, b_2 \in C^1(\bar{\Omega})$ and satisfy $b_1(X) \geq \underline{b}$ and $b_2(X) \geq \underline{b}$ in Ω for some positive constant \underline{b} . We also assume that $\lambda, f \in L^2(\Omega)$. Finally, for simplicity, we assume that $\partial\Omega$ is polygonal to avoid discussion on approximation of curved boundaries.

Let Ω be partitioned into a triangular mesh. For an arbitrary triangle T in the mesh with vertices X_i, X_j, X_k , the standard linear basis functions φ_i, φ_j and φ_k satisfy

$$\varphi_l(X_m) = \delta_{lm} \quad (4.3)$$

for $l, m = i, j, k$, where δ_{lm} denotes the Kronecker delta. Similarly to the 1D case, we define the weight $m_l(X)$ corresponding to $\varphi_l(X)$ as

$$m_l(X) = B(-(A_\varepsilon^{-1} \mathbf{b})^t (X - X_l)).$$

Using these weights, we obtain the following weighted basis functions on T :

$$\tilde{\varphi}_l = \frac{m_l(X) \varphi_l}{m_i(X) \varphi_i + m_j(X) \varphi_j + m_k(X) \varphi_k}, \quad l = i, j, k, \quad (4.4)$$

where each $\tilde{\varphi}_l$ has the same support as φ_l . Using (4.3) and the definition of $\tilde{\varphi}_l$, it is easy to show that $\tilde{\varphi}_l$ ($l = i, j, k$) satisfy the following properties.

Lemma 4.1. *The weighted basis function is continuous and satisfies that*

$$\tilde{\varphi}_l(X_m) = \delta_{lm}, \quad 0 \leq \tilde{\varphi}_l \leq 1,$$

for $l, m = i, j, k$ and

$$\tilde{\varphi}_i + \tilde{\varphi}_j + \tilde{\varphi}_k = 1$$

on \bar{T} .

Remark 4.1. If $m_l(X) (l = i, j, k)$ are identical, then $\tilde{\varphi}_i$ reduces to φ_i , and

$$\text{Span}\{\tilde{\varphi}_i, \tilde{\varphi}_j, \tilde{\varphi}_k\} = \text{Span}\{\varphi_i, \varphi_j, \varphi_k\}. \tag{4.5}$$

Otherwise, statement (4.5) does not hold. However, we still have

$$P_0 \subset \text{Span}\{\tilde{\varphi}_i, \tilde{\varphi}_j, \tilde{\varphi}_k\}.$$

For every $\tilde{\varphi}_l (l = i, j, k)$ we define a flux \mathbf{g}_l by

$$\mathbf{g}_l = -A_\varepsilon \nabla \tilde{\varphi}_l + \mathbf{b} \tilde{\varphi}_l. \tag{4.6}$$

As in the 1D case, using (2.15) we can derive, approximations $\bar{\mathbf{g}}_i$ to \mathbf{g}_i as given below:

$$\bar{\mathbf{g}}_i = -A_\varepsilon \begin{pmatrix} x - x_j & y - y_j \\ x - x_k & y - y_k \end{pmatrix}^{-1} \begin{pmatrix} B((A_\varepsilon^{-1} \mathbf{b})^t (X - X_j)) \\ B((A_\varepsilon^{-1} \mathbf{b})^t (X - X_k)) \end{pmatrix} \tilde{\varphi}_i(X).$$

Let S_T be the measure of T for the case when X_i, X_j and X_k are arranged in the anti-clockwise direction and minus measure of S_T for the other case. Then we have

$$(x - x_i)(y - y_k) - (x - x_k)(y - y_j) = 2S_T \varphi_i(X).$$

By means of the above equality, $\bar{\mathbf{g}}_i$ can be rewritten as

$$\bar{\mathbf{g}}_i = -(A_\varepsilon / 2S_T) \begin{pmatrix} y - y_k & -(y - y_j) \\ -(x - x_k) & x - x_j \end{pmatrix} \begin{pmatrix} B((A_\varepsilon^{-1} \mathbf{b})^t (X - X_j)) \\ B((A_\varepsilon^{-1} \mathbf{b})^t (X - X_k)) \end{pmatrix} [\tilde{\varphi}_i(X) / \varphi_i(X)]. \tag{4.7}$$

Similarly, we have

$$\bar{\mathbf{g}}_j = -(A_\varepsilon / 2S_T) \begin{pmatrix} y - y_i & -(y - y_k) \\ -(x - x_i) & x - x_k \end{pmatrix} \begin{pmatrix} B((A_\varepsilon^{-1} \mathbf{b})^t (X - X_k)) \\ B((A_\varepsilon^{-1} \mathbf{b})^t (X - X_i)) \end{pmatrix} [\tilde{\varphi}_j(X) / \varphi_j(X)], \tag{4.8}$$

$$\bar{\mathbf{g}}_k = -(A_\varepsilon / 2S_T) \begin{pmatrix} y - y_j & -(y - y_i) \\ -(x - x_j) & x - x_i \end{pmatrix} \begin{pmatrix} B((A_\varepsilon^{-1} \mathbf{b})^t (X - X_i)) \\ B((A_\varepsilon^{-1} \mathbf{b})^t (X - X_j)) \end{pmatrix} [\tilde{\varphi}_k(X) / \varphi_k(X)]. \tag{4.9}$$

Noting that

$$B(-z) \equiv z + B(z), \tag{4.10}$$

we then have the following lemma.

Lemma 4.2. For any $X \in \bar{T}$, the fluxes \mathbf{g}_l and their approximations $\bar{\mathbf{g}}_l (l = i, j, k)$ satisfy

$$\mathbf{g}_i + \mathbf{g}_j + \mathbf{g}_k = \mathbf{b}, \tag{4.11}$$

$$\bar{\mathbf{g}}_i + \bar{\mathbf{g}}_j + \bar{\mathbf{g}}_k = \mathbf{b}. \tag{4.12}$$

Proof. Since $\tilde{\varphi}_i + \tilde{\varphi}_j + \tilde{\varphi}_k = 1$, we have

$$\mathbf{g}_i + \mathbf{g}_j + \mathbf{g}_k = -A_\varepsilon \nabla (\tilde{\varphi}_i + \tilde{\varphi}_j + \tilde{\varphi}_k) + \mathbf{b} (\tilde{\varphi}_i + \tilde{\varphi}_j + \tilde{\varphi}_k) = \mathbf{b}.$$

Summing (4.7), (4.8) and (4.9) and using (4.4) we obtain

$$\begin{aligned} \bar{\mathbf{g}}_i + \bar{\mathbf{g}}_j + \bar{\mathbf{g}}_k &= \frac{-A_\varepsilon}{2S_T[m_i(X)\varphi_i + m_j(X)\varphi_j + m_k(X)\varphi_k]} \\ &\times \left[\begin{pmatrix} y - y_k & -(y - y_j) \\ -(x - x_k) & x - x_i \end{pmatrix} \begin{pmatrix} B((A_\varepsilon^{-1}\mathbf{b})^t(X - X_j)) \\ B((A_\varepsilon^{-1}\mathbf{b})^t(X - X_k)) \end{pmatrix} m_i(X) \right. \\ &+ \begin{pmatrix} y - y_i & -(y - y_k) \\ -(x - x_i) & x - x_k \end{pmatrix} \begin{pmatrix} B((A_\varepsilon^{-1}\mathbf{b})^t(X - X_k)) \\ B((A_\varepsilon^{-1}\mathbf{b})^t(X - X_i)) \end{pmatrix} m_j(X) \\ &\left. + \begin{pmatrix} y - y_j & -(y - y_i) \\ -(x - x_j) & x - x_i \end{pmatrix} \begin{pmatrix} B((A_\varepsilon^{-1}\mathbf{b})^t(X - X_i)) \\ B((A_\varepsilon^{-1}\mathbf{b})^t(X - X_j)) \end{pmatrix} m_k(X) \right]. \end{aligned}$$

Using (4.10), we have

$$B((A_\varepsilon^{-1}\mathbf{b})^t(X - X_l)) = -(A_\varepsilon^{-1}\mathbf{b})^t(X - X_l) + m_l(X), \quad l = i, j, k.$$

Therefore,

$$\begin{aligned} \bar{\mathbf{g}}_i + \bar{\mathbf{g}}_j + \bar{\mathbf{g}}_k &= \frac{A_\varepsilon}{2S_T[m_i(X)\varphi_i + m_j(X)\varphi_j + m_k(X)\varphi_k]} \\ &\times \left[\begin{pmatrix} y - y_k & -(y - y_j) \\ -(x - x_k) & x - x_i \end{pmatrix} \begin{pmatrix} (A_\varepsilon^{-1}\mathbf{b})^t(X - X_j) + m_j(X) \\ (A_\varepsilon^{-1}\mathbf{b})^t(X - X_k) + m_k(X) \end{pmatrix} m_i(X) \right. \\ &+ \begin{pmatrix} y - y_i & -(y - y_k) \\ -(x - x_i) & x - x_k \end{pmatrix} \begin{pmatrix} (A_\varepsilon^{-1}\mathbf{b})^t(X - X_k) + m_k(X) \\ (A_\varepsilon^{-1}\mathbf{b})^t(X - X_i) + m_i(X) \end{pmatrix} m_j(X) \\ &\left. + \begin{pmatrix} y - y_j & -(y - y_i) \\ -(x - x_j) & x - x_i \end{pmatrix} \begin{pmatrix} (A_\varepsilon^{-1}\mathbf{b})^t(X - X_i) + m_i(X) \\ (A_\varepsilon^{-1}\mathbf{b})^t(X - X_j) + m_j(X) \end{pmatrix} m_k(X) \right] \\ &= \frac{A_\varepsilon}{m_i(X)\varphi_i + m_j(X)\varphi_j + m_k(X)\varphi_k} [A_\varepsilon^{-1}\mathbf{b}m_i(X)\varphi_i + A_\varepsilon^{-1}\mathbf{b}m_j(X)\varphi_j \\ &\quad + A_\varepsilon^{-1}\mathbf{b}m_k(X)\varphi_k] = \mathbf{b}. \end{aligned}$$

This completes the proof of this lemma. \square

Let \mathbf{e}_{pq} ($p, q = i, j, k, q \neq p$) denote the unit vector along $\overline{X_p X_q}$ and s be the length of $X_p X$ where $X \in \overline{X_p X_q}$. Putting

$$\begin{aligned} b_{pq}(s) &= (A_\varepsilon^{-1}\mathbf{b}(s))^t \mathbf{e}_{pq}, \\ d_{pq}(s) &= (A_\varepsilon^{-1}\bar{\mathbf{g}}_i(s))^t \mathbf{e}_{pq}, \end{aligned} \tag{4.13}$$

then, we have the following estimates.

Theorem 4.3. *Let $X \in \partial T$, the boundary of T . Then it holds that*

$$-\tilde{\varphi}'_i(s) + b_{pq}(s)\tilde{\varphi}(s) = d_{pq}(s)[1 + (b'_{pq}(s)/b_{pq}(s))\mathcal{O}(h)], \tag{4.14}$$

where h is the mesh parameter. Furthermore, at the vertices of T we have

$$[-A_\varepsilon \nabla \tilde{\varphi}_i + \mathbf{b}\tilde{\varphi}_i]|_{X=X_m} = \bar{\mathbf{g}}_i|_{X=X_m}, \quad m = i, j, k. \tag{4.15}$$

Before proving this theorem, we comment that this theorem provides the estimates on the difference between the fluxes and their approximations. In particular, (4.15) implies that the fluxes are equal to their approximations at the vertices of an element. This is similar to that in [27] for a different type of basis functions. This equality will later be used in the evaluation of integrals in the stiffness matrix to reduce the computational cost. Let us now prove this theorem.

Proof. If $X \in \overline{X_j X_k}$, then $\tilde{\varphi}_i(X) = 0$. Therefore, $\varphi'_i(s) = 0$, where $s = |X_j X|$. On the other hand, (4.7) can be rewritten as

$$\begin{pmatrix} x - x_j & y - y_j \\ x - x_k & y - y_k \end{pmatrix} A_\varepsilon^{-1} \mathbf{g}_i = - \begin{pmatrix} B((A_\varepsilon^{-1} \mathbf{b})^t (X - X_j)) \\ B((A_\varepsilon^{-1} \mathbf{b})^t (X - X_k)) \end{pmatrix} \tilde{\varphi}_i(X) = 0. \tag{4.16}$$

This implies that $d_{jk}(s) = 0$. Therefore, (4.14) holds for this case.

For the case $X \in \overline{X_i X_j}$, we set $s = |X_i X|$. From the definition of weighted basis function (4.4), we have

$$\tilde{\varphi}_i(s) = \frac{B(-b_{ij}s)(h_{ij} - s)}{B(-b_{ij}s)(h_{ij} - s) + B(b_{ij}(h_{ij} - s))s} = \frac{e^{b_{ij}h_{ij}} - e^{b_{ij}s}}{e^{b_{ij}h_{ij}} - 1}, \tag{4.17}$$

for $X \in \overline{X_i X_j}$, where h_{ij} denotes the length of the edge $\overline{X_i X_j}$. From the first equation of (4.16), $d_{ij}(X)$ ($X \in \overline{X_i X_j}$) can also be expressed in terms of s by using $X - X_j = -(h_{ij} - s)\mathbf{e}_{ij}$, i.e.,

$$d_{ij}(s) = \frac{1}{h_{ij} - s} B(b_{ij}(s)(h_{ij} - s)) \tilde{\varphi}_i(s) = \frac{e^{b_{ij}h_{ij}}}{e^{b_{ij}h_{ij}} - 1} b_{ij}. \tag{4.18}$$

Then, by direct computation we have

$$\tilde{\varphi}'_i(s) - b_{ij} \tilde{\varphi}_i(s) + d_{ij} = R(s) b'_{ij}, \tag{4.19}$$

where

$$R(s) = \frac{(e^{b_{ij}s} - 1)e^{b_{ij}h_{ij}} h_{ij}}{(e^{b_{ij}h_{ij}} - 1)^2} - \frac{e^{b_{ij}s} s}{e^{b_{ij}h_{ij}} - 1}.$$

It is easy to see that

$$R(0) = R(h_{ij}) = 0 \tag{4.20}$$

and

$$|R(s)| \leq c_0 \left| \frac{d_{ij}}{b_{ij}} \right| h_{ij}. \tag{4.21}$$

Here (4.18) is used to obtain the above inequality and c_0 is independent of ε and h_{ij} . Combining (4.21) with (4.19), we get

$$-\tilde{\varphi}'_i(s) + b_{ij} \tilde{\varphi}_i(s) = d_{ij} \left[1 + O\left(\frac{b'_{ij}}{b_{ij}} h_{ij}\right) \right] \quad \text{if } X \in \overline{X_i X_j}.$$

The fact that $R(0) = 0$ in (4.20) implies that

$$-\tilde{\varphi}'_i(0) + b_{ij}(0) \tilde{\varphi}_i(0) = d_{ij}(0).$$

By (4.13) we have

$$\left[-\frac{d\tilde{\varphi}_i}{d\mathbf{e}_{ij}} + (A_\varepsilon^{-1}\mathbf{b})^t \mathbf{e}_{ij} \tilde{\varphi}_i \right]_{X=X_i} = [(A_\varepsilon^{-1}\bar{\mathbf{g}}_i)^t \mathbf{e}_{ij}]_{X=X_i}. \quad (4.22)$$

Analogously, for $X \in \overline{X_i X_k}$ and $s = |X_i X|$ we also obtain

$$-\tilde{\varphi}'_i(s) + b_{ik} \tilde{\varphi}_i(s) = d_{ik} \left[1 + \mathcal{O}\left(\frac{b'_{ik}}{b_{ik}} h_{ik}\right) \right]$$

and

$$\left[-\frac{d\tilde{\varphi}_i}{d\mathbf{e}_{ik}} + (A_\varepsilon^{-1}\mathbf{b})^t \mathbf{e}_{ik} \tilde{\varphi}_i \right]_{X=X_i} = [(A_\varepsilon^{-1}\bar{\mathbf{g}}_i)^t \mathbf{e}_{ik}]_{X=X_i}. \quad (4.23)$$

Since \mathbf{e}_{ij} and \mathbf{e}_{ik} are linearly independent, combining (4.22) with (4.23) we obtain

$$\left[-A_\varepsilon \nabla \tilde{\varphi}_i + \mathbf{b} \tilde{\varphi}_i \right]_{X=X_m} = \bar{\mathbf{g}}_i|_{X=X_m}, \quad m = i.$$

Similarly, the rest of this theorem can be proved. \square

Remark 4.2. The ideas of constructing the weighted basis functions, fluxes and their approximations defined in (4.4), (4.6) and (4.7)–(4.9) can be extended to higher dimensions easily. In higher dimensional cases, Lemma 4.2 and Theorem 4.3 also hold. However, more complicated notation and symbols are needed. In this work, only a simple boundary condition, i.e., the homogeneous Dirichlet condition are considered, but this method can be applied to solve singularly perturbed convection–diffusion problems with more complex boundary conditions by using the analogous treatment in the conventional finite element method.

Let N denote the total number of mesh nodes in Ω and $V_h = \text{span}\{\tilde{\varphi}_1, \tilde{\varphi}_2, \dots, \tilde{\varphi}_N\} \subset H_0^1(\Omega)$, where $H_0^1(\Omega) := \{v : v, \frac{\partial v}{\partial x}, \frac{\partial v}{\partial y} \in L^2(\Omega), v|_{\partial\Omega} = 0\}$. The finite element method with weighted basis functions for (4.1) is to find a $w_h = \sum_{l=1}^N w_l \tilde{\varphi}_l \in V_h$ such that for any $v_h \in V_h$,

$$G(w_h, v_h) = F(v_h), \quad (4.24)$$

where

$$G(w_h, v_h) = \int_{\Omega} \{[\varepsilon_1(w_h)_x - b_1(X)w_h](v_h)_x + [\varepsilon_2(w_h)_y - b_2(X)w_h](v_h)_y + \lambda w_h v_h\} dx dy,$$

$$F(v_h) = \int_{\Omega} f v_h dx dy.$$

Using (4.2) we can easily show that the bilinear form $G(\cdot, \cdot)$ satisfies

$$G(v_h, v_h) \geq \min(\varepsilon_1, \varepsilon_2)(\nabla v_h, \nabla v_h) + \left(\left(\frac{1}{2} \nabla \cdot \mathbf{b} + \lambda \right) v_h, v_h \right) \quad \forall v_h \in V_h.$$

The above inequality implies that $G(\cdot, \cdot)$ is coercive on $V_h \times V_h$. Therefore, by the well-known Lax–Milgram theorem, there exists a unique solution to (4.24).

Setting that $w_h = \sum_{l=1}^N w_l \tilde{\varphi}_l$ and test function $v_h = \tilde{\varphi}_m$ ($m = 1, 2, \dots, N$) in (4.24), we obtain the following linear system:

$$(q_{lm})_{N \times N} (w_1, w_2, \dots, w_N)^t = \mathbf{c},$$

where \mathbf{c} is a known vector, and

$$q_{lm} = \int_{V_m} (-\mathbf{g}_l) \cdot \nabla \tilde{\varphi}_m \, dx \, dy + \int_{V_m} \lambda(X) \tilde{\varphi}_l \tilde{\varphi}_m \, dx \, dy. \tag{4.25}$$

In (4.25), V_m denotes the support of $\tilde{\varphi}_m$ that equals the union of the triangles sharing the mesh node X_m . When ε is small, $\nabla \tilde{\varphi}_m$ varies sharply along one side of an element, which makes the numerical evaluation of (4.25) difficult. To overcome this difficulty, we observe that $(\varepsilon_1(\tilde{\varphi}_l)_x - b_1\tilde{\varphi}_l, \varepsilon_2(\tilde{\varphi}_l)_y - b_2\tilde{\varphi}_l)^t$ can be approximated by $-\bar{\mathbf{g}}_l$ from Theorem 4.3, and $\bar{\mathbf{g}}_{l,1}$ and $\bar{\mathbf{g}}_{l,2}$ vary smoothly in any element T by contrast with $\nabla \tilde{\varphi}_m$. Therefore, we may approximate q_{ml} by

$$q_{lm} \simeq \sum_{T \in V_m} (-\bar{\mathbf{g}}_l(X_T))^t \cdot \int_T \nabla \tilde{\varphi}_m \, dx \, dy + \int_{V_m} \lambda(X) \tilde{\varphi}_l \tilde{\varphi}_m \, dx \, dy,$$

where $\bar{\mathbf{g}}_l(X_T)$ is the average of $\bar{\mathbf{g}}_l(X)$ at three vertices of the element T . Now, integrating by parts we get

$$q_{lm} \simeq \sum_{T \in V_m} (-\bar{\mathbf{g}}_l(X_T))^t \cdot \int_{\partial T} \mathbf{n} \tilde{\varphi}_m \, ds + \int_{V_m} \lambda(X) \tilde{\varphi}_l \tilde{\varphi}_m \, dx \, dy, \tag{4.26}$$

where \mathbf{n} is the unit outward normal vector of ∂T . The line integral in (4.26) can be numerically evaluated by (4.17) easily.

5. Numerical results

Example 1. we consider the following 1D problem:

$$-\varepsilon w' + (1+x)w' + 2w = 1, \quad 0 < x < 1, \tag{5.1}$$

with the boundary conditions

$$w(0) = w(1) = 0.$$

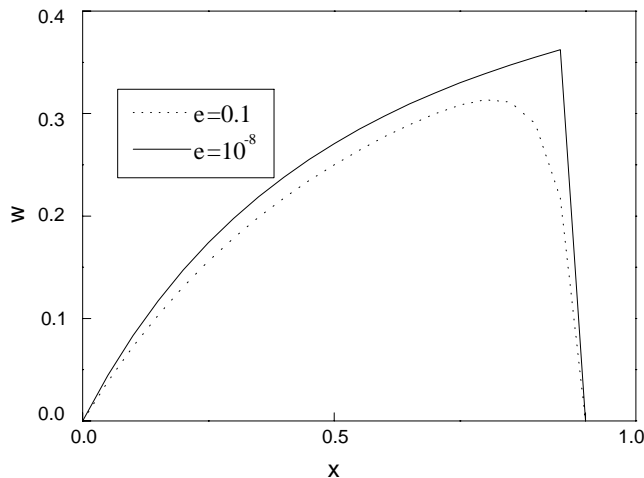


Fig. 3. Numerical solutions for $\varepsilon = 0.1$ and 10^{-8} .

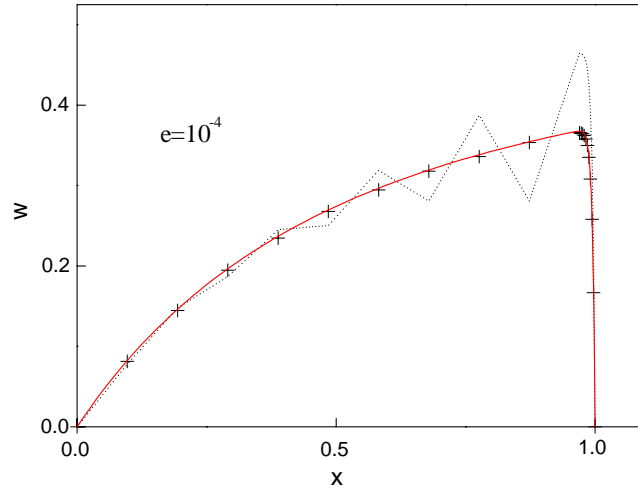


Fig. 4. The numerical solutions on a Shishkin mesh.

To solve this problem we choose a uniform mesh with $N = 30$ and apply the method with weighted basis functions on this mesh to two cases: $\varepsilon = 10^{-1}$ and $\varepsilon = 10^{-8}$. Numerical results displayed in Fig. 3 demonstrate that this method is stable for the chosen values of ε .

To test the second-order method, we solve (5.1) on a Shishkin mesh (cf. for example, [17]) by two methods. One is the conventional piecewise linear finite element method, and the other is the mixed method obtained by applying the finite element method with basis functions in a subregion containing the boundary layers and the piecewise linear finite element method in the rest of the domain. In our computation, $N = 20$, $\tau_0 = 2$ and $\varepsilon = 10^{-4}$. The results are plotted in Fig. 4 in which the solid line denotes the exact solution to (5.1), and + and dot denote the numerical solutions obtained by the mixed method and the linear finite

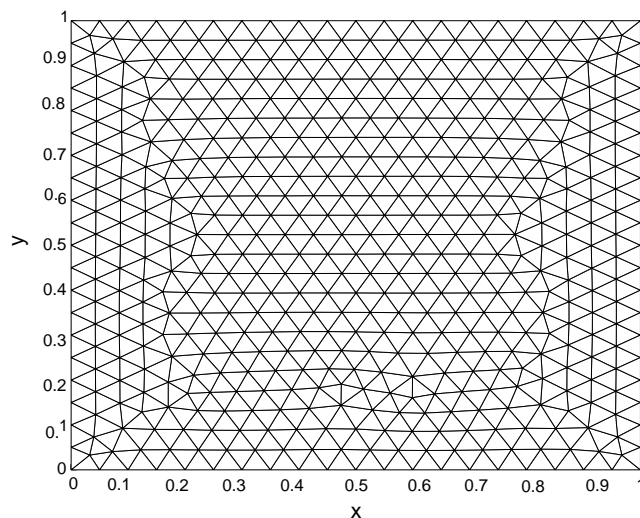


Fig. 5. The triangulation of $(0, 1)^2$.

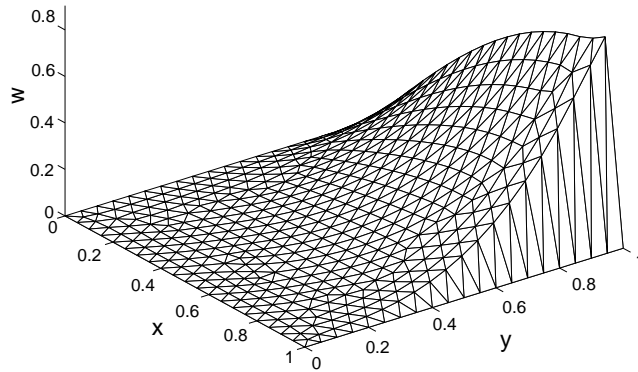


Fig. 6. The computed solution of Example 2.

element method, respectively. From Fig. 4 we see that the solution from the linear finite element method contains spurious oscillations even on the Shishkin mesh, while the solution from the mixed method matches the exact one very well.

Example 2. Let us consider the 2D singular perturbation problem defined by

$$\begin{aligned} \nabla \cdot \begin{pmatrix} -\varepsilon_1 w_x + (3-x)w \\ -\varepsilon_2 w_y + (4-2y+y^2)w \end{pmatrix} + (4-2y)w = f(x,y), \quad (x,y) \in \Omega, \\ w|_{\partial\Omega} = 0, \end{aligned} \tag{5.2}$$

where $\Omega = (0, 1)^2$ and

$$f(x,y) = \frac{3}{2}\pi \cos \frac{\pi x}{2} + y^3 \sin \frac{\pi x}{2} - \frac{\pi x}{2} \cos \frac{\pi x}{2} + 12y^2 - 6y^3 + 3y^4.$$

In our computation, we choose $\varepsilon_1 = 10^{-3}$ and $\varepsilon_2 = 10^{-6}$. The triangulation of the computational region is displayed in Fig. 5 with 930 elements and 506 nodes. We solve (5.2) by the weighted finite element method and the numerical solution is depicted in Fig. 6. Clearly, the figure shows that this method is stable and convergent.

6. Concluding remarks

In this paper we present a finite element method for a singularly perturbed convection–diffusion problem. The method is based on a set of weighted basis functions. The method is described in both one and two dimensions. For the one dimensional case, both first-order and second-order methods are given. In fact, the 1D method is similar to the an existing Petrov–Galerkin method based on \bar{L}^* -splines (cf. for example, Section 2.2 of [22]), though it is a Bubnov–Gerlerkin method.

The 1D first-order scheme is extended to two dimensions, based on an unstructured triangular mesh. Theoretical investigations on the properties of the basis functions are performed. We comment that the method in two dimensions is a Bubnov–Galerkin method since the test and trial function spaces are identical in the method.

Numerical examples are also solved to show the usefulness of the method. The numerical results demonstrate that this method is stable and convergent when sharp boundary layers are present.

Acknowledgements

This work was partially supported by the Research Committee of The Hong Kong Polytechnic University (Project Account Code: G-T609). The third author (SW) wishes to acknowledge the support from the Australian Research Council.

References

- [1] O. Axelsson, Stability and error estimates of Galerkin finite element approximations for convection–diffusion equations, *IMA J. Numer. Anal.* 1 (1981) 329–345.
- [2] R. Bank, J.B. Bürger, W. Fichtner, R. Smith, Some up-winding techniques for finite element approximations of convection diffusion equation, *Numer. Math.* 58 (1990) 185–202.
- [3] T. Belytschko, I. Eldib, Analysis of a finite element upwind scheme, in: AMD, vol. 34, Am. Soc. Mech. Eng., New York, 1979, pp. 195–200.
- [4] A.N. Brooks, T.J.R. Hughes, Streamline upwind Petrov–Galerkin formulations for convection dominated flows with particular emphasis on the incompressible Navier–Stokes equations, *Comput. Methods Appl. Mech. Eng.* 32 (1982) 199–259.
- [5] I. Christie, D.F. Griffiths, A.R. Mitchell, Finite element methods for second order differential equations with significant first derivatives, *Int. J. Numer. Methods Eng.* 10 (1976) 1389–1396.
- [6] I. Christie, A.R. Mitchell, Upwinding of high order Galerkin methods in conduction–convection problems, *Int. J. Numer. Methods Eng.* 12 (1978) 1764–1771.
- [7] B. Cockburn, C.-W. Shu, The local discontinuous Galerkin method for time-dependent convection–diffusion systems, *SIAM J. Numer. Anal.* 35 (1998) 2440–2463.
- [8] B. Cockburn, C.-W. Shu, TVB Runge–Kutta Local projection discontinuous Galerkin finite element method for conservation laws II: general framework, *Math. Comput.* 52 (1989) 411–435.
- [9] D.F. Griffiths, On the approximation of convection problems in fluid dynamics, *Int. J. Numer. Methods Eng.* 11 (1977) 1477–1483.
- [10] J.C. Heinrich, O.C. Zienkiewicz, Quadratic finite element schemes for two-dimensional convection-transport problems, *Int. J. Numer. Methods Eng.* 11 (1977) 1831–1844.
- [11] J.C. Heinrich, O.C. Zienkiewicz, The finite element method and ‘upwinding’ techniques in the numerical solution of convection dominated flow problems, in: AMD, vol. 34, Am. Soc. Mech. Eng., New York, 1979, pp. 105–136.
- [12] P.W. Hemker, A numerical study of stiff two-point boundary problems, PhD Thesis, Mathematical Centre, Amsterdam, 1979.
- [13] T.J.R. Hughes, Multiscale phenomena: Greens functions, the Dirichlet–Neumann formulation, subgrid scale models, bubbles and the origins of stabilized methods, *Comput. Methods Appl. Mech. Eng.* 127 (1995) 387–401.
- [14] T.J.R. Hughes, A simple scheme for developing ‘upwind’ finite elements, *Int. J. Numer. Methods Eng.* 12 (1978) 1359–1365.
- [15] T.J.R. Hughes, A. Brooks, A multi-dimensional upwind scheme with no crosswind diffusion, in: AMD, vol. 34, Am. Soc. Mech. Eng., New York, 1979, pp. 19–35.
- [16] J. Johnson, Numerical solution of partial differential equations by the finite element method, Cambridge University Press, Cambridge, MA, 1987.
- [17] J.J.H. Miller, E. O’Riordan, G.I. Shishkin, Fitted numerical methods for singular perturbation problem, World Scientific, Singapore, 1996.
- [18] J.J.H. Miller, S. Wang, A new non-conforming Petrov–Galerkin method with triangular elements for a singularly perturbed advection–diffusion problem, *IMA J. Numer. Anal.* 14 (1994) 257–276.
- [19] J.J.H. Miller, S. Wang, An exponentially fitted finite element volume method for the numerical solution of 2D unsteady incompressible flow problems, *J. Comput. Phys.* 115 (1994) 56–64.
- [20] E. O’Riordan, M. Stynes, A global uniformly convergent finite element method for a singularly perturbed elliptic problem in two dimensions, *Math. Comput.* 57 (1991) 47–62.
- [21] H.-G. Roos, Layer-adapted grids for singular perturbation problems, *Z. Angew. Math. Mech.* 78 (1998) 291–309.
- [22] H.-G. Roos, M. Stynes, L. Tobiska, Numerical methods for singularly perturbed differential equation, Springer, Berlin, 1996.
- [23] M. Stynes, E. O’Riordan, A finite element method for a singularly perturbed boundary value problem, *Numer. Math.* 50 (1986) 1–15.
- [24] M. Stynes, E. O’Riordan, An analysis of a singularly perturbed two-point boundary value problem using only finite element techniques, *Math. Comput.* 56 (1991) 663–675.
- [25] G. Sun, M. Stynes, Finite element methods for singularly perturbed higher order elliptic two-point boundary value problems I: reaction–diffusion type, *IMA J. Numer. Anal.* 15 (1995) 117–139.

- [26] S. Wang, A novel exponentially fitted triangular finite element method for an advection–diffusion problem with boundary layers, *J. Comput. Phys.* 134 (1997) 253–260.
- [27] S. Wang, Z.C. Li, An analysis of a conforming exponentially fitted triangular finite element method for a singularly perturbed convection–diffusion equation, *J. Comput. Appl. Math.* 143 (2002) 291–310.
- [28] S. Wang, Z.C. Li, A non-conforming combination of the finite element and volume methods with an anisotropic mesh refinement for a singularly perturbed convection–diffusion equation, *Math. Comput.* 72 (2003) 1689–1709.
- [29] J. Xu, L. Zikatanov, A monotone finite element scheme for convection–diffusion equations, *Math. Comput.* 68 (1999) 1429–1446.